Investigation on the structure-electrical property relationship of hydrolyzed poly(vinyl alcohol) membranes

J.F. Jurado[a], O. Checa[a] and, R.A. Vargas[b]

[a] *Departamento de Física y Química, Universidad Nacional de Colombia,*
A.A 127, Manizales, Colombia
e-mail: jfjurado@unal.edu.co
[b]*Departamento de Física, Universidad del Valle,*
A.A. 25360, Cali, Colombia.

This investigation explored the effects of the pre-treatment temperature on the molecular conformations and electrical performance of poly(vinyl alcohol) (PVOH) membranes. The structure and properties of the membranes were characterized by X-ray diffraction (XRD), differential scanning calorimetry (DSC), thermogravimetric analysis (TGA), Raman scattering (RS) and impedance measurements (IE). Water molecules absorbed by the PVOH membranes, which decreased in quantity as the temperature increased caused drastic change to be observed in the relative band intensities of the OH and CH_2 bonds with respect to the C-C bonds. The observations for the hydrated PVOH were correlated with the proton transport behavior, which were inferred from conductivity relaxation measurements over various temperature regions and were dependent on the water content in the membrane. The results were corroborated by DSC and TGA. For example, the temperature dependence of the conductivity relaxation frequency, ω_{max}, followed different Arrhenius-type thermally activated processes at low and high temperatures. The corresponding activation energies in the low and high temperature regions were: 1.42 ± 0.02 and 0.23 ± 0.02 eV, respectively. In addition, the selected fitting temperature regions and activation energies for the ω_{max} data were equivalent (within experimental error) to the values for the dc-conductivity, $\sigma_0(T)$. This result indicates that the mechanisms for long range ion displacement (dc conductivity) and ion-ion or ion-polymer chain correlations are identical, (*i.e.*, an ion-hoping occurred in the various hydrated phases of PVOH).

Keywords: X-ray diffraction; vibrational states in disordered systems; ionic conduction; polymers.

PACS: 61.05.cp; 63.50.+x; 66.10.Ed; 66.30.hk

1. Introduction

Polymers and polymeric composites have steadily become more prevalent in our daily lives. Permanent electrical effects in both dielectrics and conductors have been utilized in a wide variety of applications. Among the materials with permanent electrical effects is poly(vinyl alcohol) (PVOH), a hydrophilic, biodegradable and non-toxic synthetic polymer, which has been widely used in different areas of research, development and production. These uses extend from technological areas (*i.e.*, fuel cells, batteries and electrochromic devices) to the biological and medical fields. The stereochemistry of the OH groups along the backbone of the chain leads to three distinct polymer configurations: isotactic (i), syndiotactic (s) and atactic (a) [1–7]. All of the OH groups lie in the same side of the plane of the extended polymer backbone in i-PVOH. The OH groups regularly alternate from one side of the plane to the other in the case of s-PVOH. However, there is no specific OH distribution for a-PVOH. Generally, all three configurations co-exist, with s-PVA as the prominent phase (up to 53-62%) content [1, 5]. The sequential distribution of OH groups on either side of the s-PVA backbone under favorable conditions can be explored to design a layered structure by bridging water molecules. PVOH-based films have been used for applications such as proton exchange membranes (PEMs) in fuel cells [5, 7]. Many desirable characteristics, such as high hydrophilicity, high me-

chanical strength and relatively low cost have attracted attention for the further development of PEMs. The degree of the absorption of water is one of the most important factors that determine the properties and applications suitable for PVOH. For example swollen PVOH-H_3PO_2 membranes, contain liquid-filled cavities that are able to absorb large amounts of electrolytes [8]. The swelling in properties of PVOH-based membranes play an important role in the electrical conductivity performance. The proton transport properties of a membrane can be improved by enhancing the hydrophilicity of the membrane because an increase in hydrophilicity increases, the selectivity of water toward organic [9] and inorganic [10–13] aqueous solutions. For example, PVOH can interact with inorganic salts and acids to enable ionic conduction in a polymer matrix. The membranes remain conducting even at high PVOH content. The hydroxyl groups attached to the polymer backbone can be a source of hydrogen bonding, which can assist with the formation of proton conducting polymers [2–4]. The conformation of the PVOH orientation of the hydroxyl groups, and chemical bonding might the surface wettability of a PVOH membrane and the interactions of the polymer chain with constitutional water molecules. In this work, based on hydrolyzed poly(vinyl alcohol) (PVOH) powders, polymer membranes were developed and characterized their ionic transport behavior as a function of temperature and electric field frequency in order to obtain information regarding the nature and types

of molecular dynamics that might explain their electrical response. In addition, the relations between the chemical composition, molecular structure and morphology were studied. The electrical responses of the membranes were compared with the Raman spectra and thermal analysis measurements to infer structure-property relationships for PVOH, which can be a precursor polymer for the development of PEMs.

2. Experimental details

2.1. Membrane preparation

Poly(vinyl alcohol) (PVOH) was purchased from Sigma-Aldrich. The average degrees of polymerization and hydrolysis were; Mw=85,000-124,000 and 87-89%, respectively. To prepare the samples, a consistent mass of polymer was dissolved in deionized water at 80°C for 24 hours with magnetic stirring to form, homogeneous solutions, which all polymer grains dissolved. The resulting gels were poured into glass plates (Petri) and stored in a dry atmosphere for several days until the gels solidified. Uniform, smooth and thin (thickness between 100 and 500 μm) membranes were obtained, which were dry to the touch and semitransparent to visible light.

2.2. Membrane characterization

The result membranes were characterized by X-ray diffraction (XRD), differential scanning calorimetry (DSC), thermogravimetric analysis (TGA), Raman scattering (RS) and impedance spectroscopy (IS). The room temperature X-ray diffraction measurements were performed with an Advance A8 Bruker AXS diffractometer, with a monochromatic radiation source Cu-K$_\alpha$ (1.5406 Å). Raman scattering measurements were performed with a LabRAM HR800 Horiba JobinYvon high-resolution spectrometer, with a laser beam spot size in 2μm the 473 nm line, over a spectral range of 150 to 4000 cm^{-1}. The crystalline sample was located in a home-made micro-furnace coupled to the micro-Raman instrument for in situ Raman spectroscopy measurements as a function of temperature. The temperature was recorded with a type-K thermocouple located very close to the sample. The Raman spectra were recorded at various isotherms over a temperature range of 25 to 120°C . The experimental temperature was maintained within ±0.5°C of the temperature-controlled micro-furnace. The thermal stabilities of the membranes were was characterized using a TA Instruments Q100 DSC. The samples mass were between 3 and 6 mg and hermetically sealed in aluminum pans. Each sample was scanned from -40 to 350°C at a heating rate of 5°C· min^{-1}, while under a 50 ml· min^{-1} flow of nitrogen gas. Thermogravimetric analysis (TGA) was performed using a TA Instruments 2050 TGA microbalance controlled by a computer. All samples were measured over a temperature range of 27 to 350°C, at a rate of 5°C· min^{-1}. Dry nitrogen was used as the purge gas. The weight of the samples varied between 20 and 40 mg. The impedance measurements were performed using a LCR meter (Wayne Kerr 6420) controlled by a computer over a the frequency range of 10 to 5 MHz with an excitation signal of 500 mV. Possible nonlinear effects due to the amplitude of the voltage were checked up to 1.0 V over the entire frequency range for the typical two-electrodes cell with a Au/membrane/Au configuration, (Novocontrol, Standard sample cell BDS 1200). The measuring cell was located in a sealed, temperature-controlled home-made chamber. An E-type thermocouple located near the PVOH polymer membrane was used for the temperature measurements. Each sample was equilibrated at the experimental temperature for at least 2 min before measurements were acquired. The impedances of the membranes were recorded at various isotherms over a temperature range of 24 and 200°C . The experimental temperatures were maintained within ±0.5°C . At least three measurements for each experiment were acquired for each polymer membranes.

3. Results and discussion

3.1. X-ray diffraction

A typical XRD profile of a PVOH membrane at room temperature is shown in Fig. 1, showing broad peaks attributed to combination of amorphous and crystalline regions in the sample. By assuming that the crystalline phase had a monoclinic structure and using the initial parameters reported by Young et al., [14, 15], the following crystallographic parameters were determined using the Xpowder fitting software: $a = 7.81$ Å, $b = 2.52$ Å (chain axis), $c = 5.51$ Å, $\beta = 91.2°$. The most intense peak, which was observed at approximately $2\theta = 22.5°$, indicated the degree of crystallinity of the membrane with an atactic polymer configuration of the OH groups, a-PVOH [14]. However, the crystalline peak at $2\theta = 22.5°$ was assigned as the diffraction from (101) crystalline plane. Each (101) plane contained extended-chain backbones, which were represented in planar zigzag conformations.
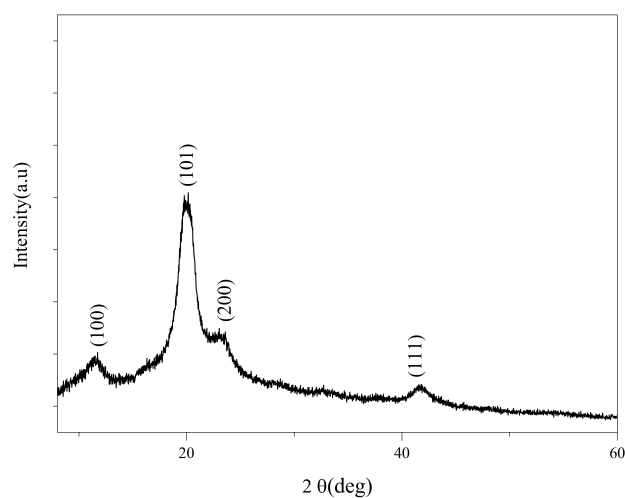

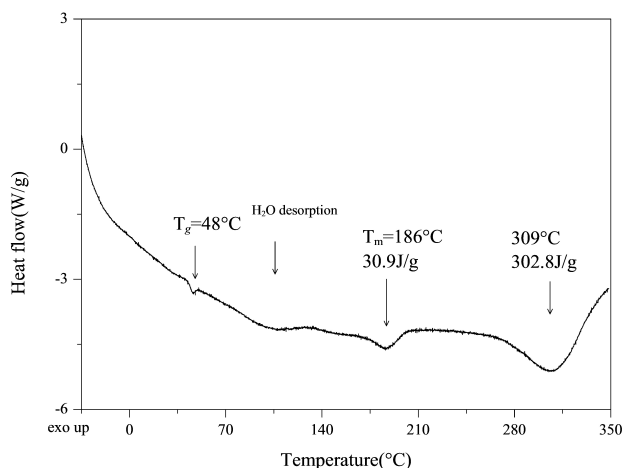FIGURE 1. X-ray diffraction at room temperature of PVOH membrane.

FIGURE 2. DSC curve for PVOH-membrane in nitrogen atmosphere at the heating rate of $5°C \cdot min^{-1}$.

FIGURE 3. TG and DTG curves for PVOH-membrane heat in nitrogen atmosphere at heating rate of $5°C \cdot min^{-1}$.

3.2. Thermal characterization (DSC and TGA) results

Figure 2 shows the DSC curve for a freshly prepared membrane of PVOH over a temperature range of -40 to $350°C$. Four thermal events were observed as the sample was heated. The first step-type event occurred at approximately $48°C$, which was associated with the glass transition of the polymer. A second broad endothermic peak was observed between approximately 60 and $140°C$, which was attributed to surface water desorption followed by partial evaporation of bound water in the polymer membrane. It should be noted that if the membrane was initially heated to $160°C$ and subsequently subjected to subsequent thermal cycle over -40 to $160°C$, then the second endothermic event was no observed. A third endothermic peak was observed at approximately $186°C$ with a change in enthalpy of 30.9 J/g, which was attributed to the melting of the crystalline components of the polymer membrane. Finally, a fourth intense peak at approximately $309°C$ with a change in enthalpy of 302.8 J/g, which was associated with the degradation of the backbone of the polymer -chain.

Figure 3 shows the TGA and differential gravimetric analysis (DTG) curves of a representative freshly prepared PVOH membrane, which was heated from 25 to $400°C$. Several weight loss regimes were observed in the TGA and DTG curves. The first region (30 to $130°C$) was attributed to the evaporation of physically (weakly) and chemically (strongly) bound water. The total weight loss of the membrane was approximately 7.43 wt.% at $130°C$. If the sample was heated at $160°C$ for 30 min prior to measurement, then the observed weight loss at this isotherm was less than 1.0 wt.%. This weight loss region was correlated with the broad endothermic peak observed in the DSC curve (Fig. 2). Upon subsequent heating of sample, a monotonically decreasing sample weight was observed above the melting point of the polymer, which occurred approximately $186°C$ according to the DSC results (Fig. 2). The maximum weight loss rates occurred at approximately 247, 306.7 and $333.5°C$. The total weight
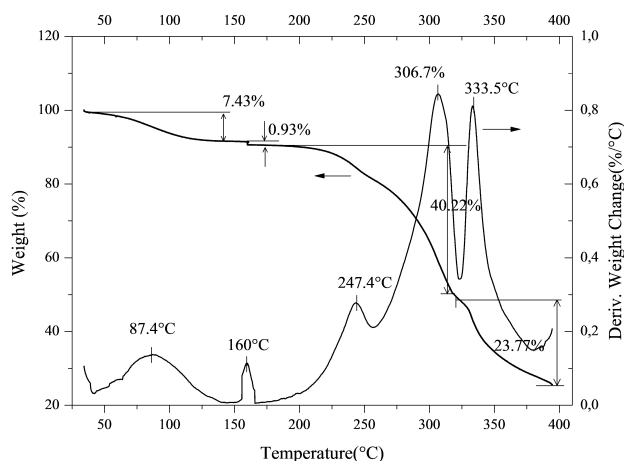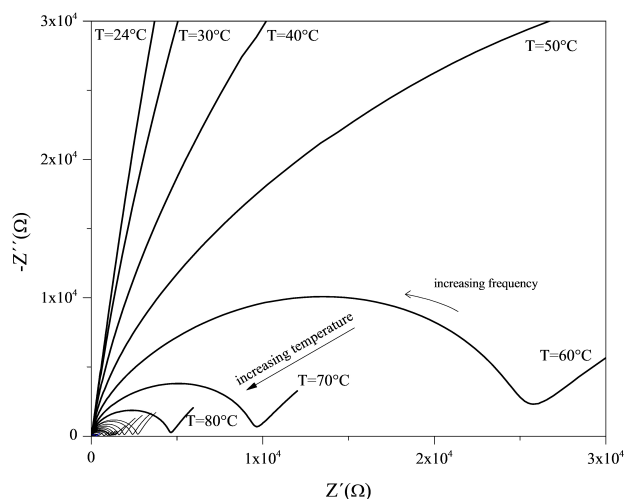

FIGURE 4. Complex Impedance (Nyquist) plots of PVOH-membrane for a range of temperature.

loss of the sample at the final heating temperature ($400°C$) was approximately 71 wt.%. The weight loss in this second heating region (180 to $400°C$)was attributed to the continuous thermal degradation of the polymer, which the maximum rate of the decomposition occurred at approximately $306.7°C$. Additionally, the DSC curve showed a prominent change in enthalpy at this temperature.

3.3. Impedance spectroscopy (IS)

Figure 4 shows several typical Nyquist ($-ImZ$ versus ReZ) plots acquired at several isotherms between 24 and $210°C$ for a representative PVOH membrane. It is important to note that a well-defined arc passing through the origin in the high frequency limit, which is related to conduction process in the bulk of the membranes, can be observed in the Nyquist plots in the operating frequency range (10 to 5 MHZ) and at temperatures higher than $50°C$. Additionally the extrapolation of

the arc to the ReZ axis which the intercept was the bulk resistance of the membrane, R decreased as the temperature increased. This result indicated that a thermally activated process occurred.

The dc conductivity, was calculated from the Nyquist plots, using the known formula, $\sigma = d/AR$, where d is the thickness, A is the contact area of the membrane and R is the bulk resistance. Figure 5 shows the temperature dependence of the dc-conductivity for the PVOH membrane. Based on a least square analysis of the corresponding data, straight lines used to fit two segments of data points, ($\log T\sigma$ vs. 1000/T) worked well. One of the segments was at low temperatures (24 to 70°C) and other segment was at high temperatures (90 to 160°C). The activation energy, E_a, was calculated from the fitting parameters according to the Arrhenius model, $T\sigma(\text{T}) = \sigma_0 e^{-E_a/k_\beta T}$, where k_β is the Boltzmann's constant and T the absolute temperature. The calculated values of E_a were; 1.42 ± 0.02 and 0.23 ± 0.02 eV for the segments of data points in the $24 - 70°$C and $90 - 160°$C temperature ranges, respectively. This change in slope is often observed in polymer electrolytes [16] and is generally attributed to a thermal change between two different elastomeric phases in the polymeric membrane. According to the DSC (Fig. 2) and TGA (Fig. 3) results, the first change occurred in the region where water content in the polymer membrane was liberated (*i.e.*, in the temperature region at approximately 80°C), while the onset temperature of the second change occurred at approximately the melting point of the membrane (186°C).

To characterize the dynamics of the diffusing ions in the PVOH membrane, the electrical relaxation relation phenomena in these membranes was analyzed [16]. Figure 6 shows typical plots of the frequency dependence of the real part of the conductivity, $\sigma'(\omega)$, for a representative membrane, which is presented in a double-logarithmic scale for several isotherms. The complex conductivity, $\sigma(\omega) = \sigma'(\omega) + i\sigma''(\omega)$, was calculated from the complex
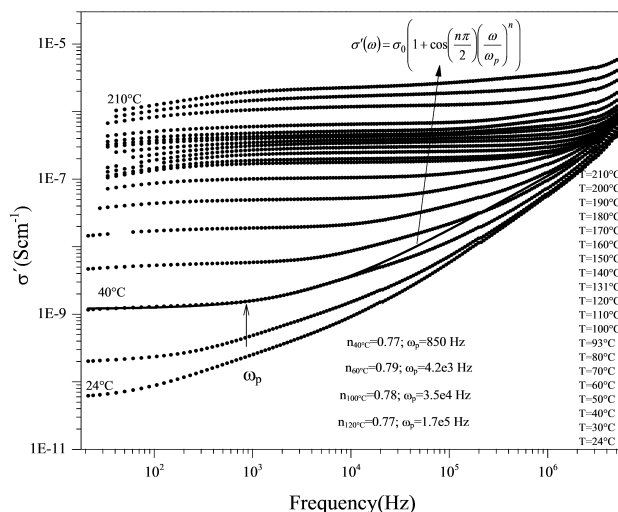
FIGURE 6. log-log plots of PVOH- membrane $\sigma'(\omega)$ data for a range of temperature. The continuous line is a representative fitting curve to the expression (1) for the conductivity spectra at T=40°C. The inset shows the fitting parameters, n and ω_p for the spectra at other isotherms.

admittance data, $Y(\omega) = 1/Z(\omega) = G(\omega) + i\omega C(\omega) = A/d\sigma(\omega)$, where G and C are the parallel conductance and capacitance, respectively. All plots were characterized in the low-frequency region by a well-developed non dispersive dc conductivity or plateau region over a wide temperature range. A decrease in the conductivity was clearly resolved at the lowest frequencies of the spectra, mainly at the highest temperatures, which may be ascribed to ionic transport processes through the sample-electrode interface. As frequency increased a crossover occurred with a power-law dependent conductivity of the form ω^n, which was evident at lower temperatures. The $\sigma'(\omega)$ is usually described by the phenomenological expression,

$$\sigma'(\omega) = \sigma_0 \left[1 + \cos\left(\frac{n\pi}{2}\right) \left(\frac{\omega}{\omega_p}\right)^n \right] \qquad (1)$$

Which is frequently observed in ionic conductors [17, 18]. The exponent, n, is usually between 0 and 1. The value is expected to be close to 1 for highly correlated ions and close to 0 for random Debye-like hops. The crossover frequency, ω_p, defines a characteristic relaxation frequency, which increases with increasing temperature, while σ_0 is the dc conductivity. The observed power-law in the conductivity at high frequencies was ascribed to a nonrandom hopping mechanism, which resulted from many body interactions among charge carriers. It is import to note that the values of σ_0 obtained by extrapolation of the dc-conductivity plateau (the low-frequency region) shown in Fig. 6 coincide (within experimental error) within the values obtained by using the values of R given by the Nyquist plots (Fig. 4) by extrapolating the circular arc to the real axis of the impedance plots. An exponent of $n=0.8\pm0.5$ was obtained from the fits using Eq. (1) over the whole temperature range. Identical results to those reported
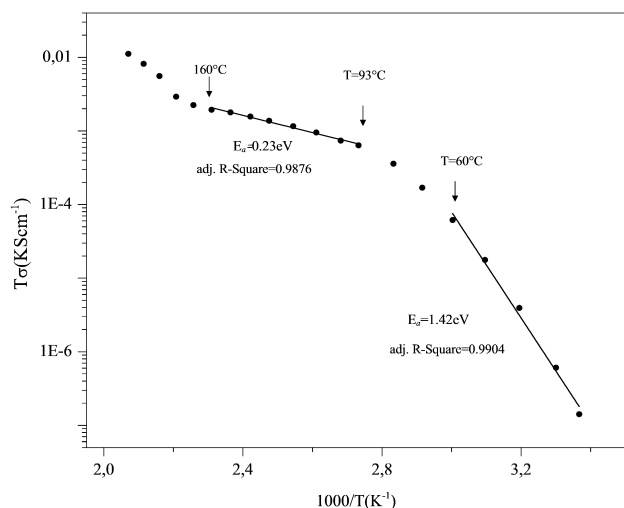

FIGURE 5. Arrhenius plot of conductivity for PVOH-membrane. The continuous lines indicate linear fit to the date points in different temperature ranges.
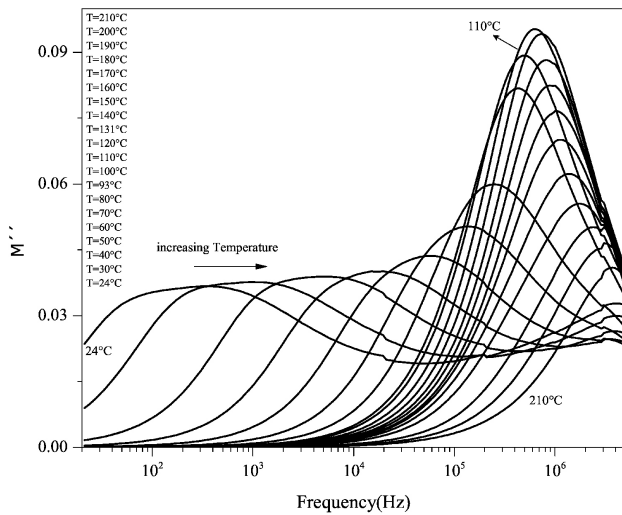
FIGURE 7. Frequency dependence of the imaginary part of the electric modulus for PVOH- membrane for a range of temperature.
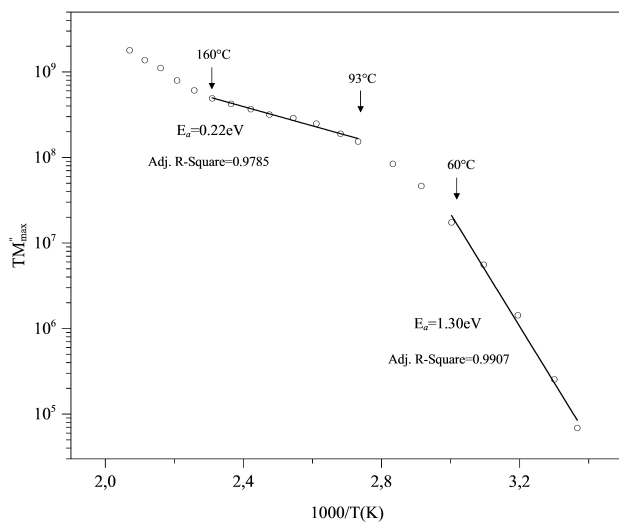

FIGURE 8. Arrhenius plot of Relaxation frequency. The continuous lines indicate linear fit to the date points in different temperature ranges.
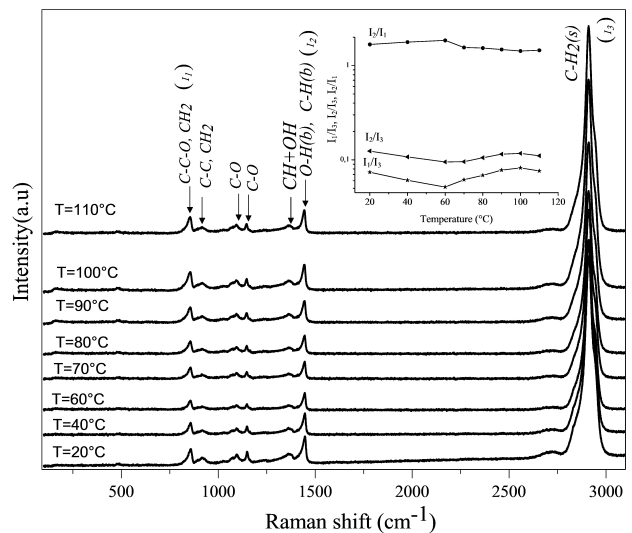

FIGURE 9. Raman spectra of PVOH-membrane at different temperatures. The arrows indicate the location of the modes, in correspondence with Ref. 24 and 25. The inset show relative band intensities.

pressed, which can otherwise become prominent at low frequencies [22]. Figure 7 shows the imaginary part of the electric modulus at various isotherms. A peak was observed with a frequency, ω_{max}, that was thermally activated (see Fig. 8). This peak marked the transition regime from long range (i.e., dc conductivity) to short range ionic mobility. The height and half width of the peaks changed abruptly through the temperature region (60 to 110°C) where the constitutional water molecules were release from the membranes. The modulus maxima of Fig. 7 decreased rapidly as the temperature increased above approximately 160°C. The dynamic processes of ionic transport that occurred over various temperature regions were different. The results were corroborated by DSC and TGA measurements. This conclusion was also evident from the asymmetric shape of the peaks.

The conductivity relaxation frequency, ω_{max}, provided the most probable relaxation time τ, according to the following condition: $\omega_{max} \cdot \tau = 1$. The temperature dependence of ω_{max} is shown in Fig. 8, which was plotted as $\ln(T\omega_{max})$ versus $1000/T$. It was noted that the plot exhibited Arrhenius-type thermally activated processes throughout two segments of data points: 24 to 80°C and 90 to 160°C. The corresponding activation energies in this two regions were 1.30 ± 0.02 and 0.22 ± 0.02 eV, respectively. The selected fitting temperature regions and activation energies for the ω_{max} data were (within experimental error) equivalent to the values determined for $\sigma_0(T)$ (see Fig. 5). This result strongly indicates that the mechanisms for long range ion displacement (dc conductivity) and ion-ion or ion-polymer chain correlations were identical (i.e., ion-hoping) [23].

3.4. Raman spectra (RS)

The Raman spectra of a representative PVOH membrane at various isotherms between 20 and 120°C are shown in Fig. 9.

for the PVOH membrane (inset Fig. 6) are frequently observed in other structurally disordered materials such as ionically conducting glasses, conducting polymers, amorphous semiconductors and doped crystalline solids [19–21]. The feature is often referred to as "universal dynamic response". These observations indicate that the charge transfer mechanisms based on ion migration mediated by either ion-ion or ion-polymer chain interactions, which are similar to mechanisms for other ionic materials, are also responsible for ionic conductivity in the PVOH membranes.

An alternative time domain image of the effects of ion-hopping correlated with relaxations in the conductivity can be obtained from the modulus formalism [22], $M(\omega)=i\omega\epsilon_0/\sigma(\omega)$, which describes the relaxation of the electric field at a constant displacement vector. The main advantage of this formalism is that the electrode effects can be sup-

The various observed active modes of the PVOH membrane were assigned in accordance with Ref. [24, 25], which were identified as stretching modes (s) and bending modes (b). The positions of the various bands were invariant as the temperature increased to approximately 120°C. However, as the ratios of the peak intensities localized at $I_1 = 855$ cm^{-1} (vibration C−C−O stretching), $I_2 = 1438$ cm^{-1} (vibration CH$_2$ bending) and $I_3 = 2912$ cm^{-1} (vibration CH$_2$ stretching), were obtain the data shown in Fig. 9 were obtained as a function, which the following relative band intensities were plotted: I_1/I_2, I_1/I_3, and I_2/I_3. The temperature dependence of the ratios was observed to have a change in curvature at approximately 60°C, which was the temperature that water began to be liberated from the membrane (see TGA results, Fig. 3). At low temperatures, the ratio of the number of excited modes corresponding to the bonds (C−C)/(C−H) and (C-C)/(O-H) decreased as the temperature increased, while the (OH)/(C−H) ratio increased. However, at temperatures above 60°C, the trend inverted and the (OH)/(C−H) ratio became almost constant. The comparison between the relative band intensities with temperature provided evidence for the effects of water molecules on the energetics of the excited modes, which mainly affected the intensity of the excited modes of the CH$_2$ bonds, (also known as "CH$_2$ rocks") and are correlated with the OH bonds for water liberation. The well-established correlation between the DSC (Fig. 2), TGA (Fig. 3), ionic conductivity (Figs. 5 and 7) and Raman scattering (Fig. 9) results indicated that the water content in the PVOH membrane, affected the dynamics of proton transport and energetics of the exited modes associated with the various modes in the PVOH polymer matrix.

As PVOH membrane was heated above 120°C, the material underwent color transition from transparent, to white-milky, to yellow, and finally, to an obscure brown coloration. The background noise of the Raman spectra also increased as the temperature increased. The positions of the bands remained invariant; however, the relative intensities of the corresponding peaks changed drastically. In addition, the modes corresponding to lower wave-numbers tended to disappear, while modes at 2912 cm^{-1} remained highly intense. The excitation of the less energetic modes was energetically unfavorable in the absence of water molecules and as the temperature was increased above 120°C. This behavior was also observed as the PVOH was held at 120°C for more than 20 min, while the Raman spectra were subsequently acquired at room temperature.

4. Conclusions

PVOH membranes prepared with a fixed water content (*i.e.*, pre-treatment temperature) were investigated using, XRD, thermal analysis (*i.e.*, DSC and TGA), IS and RS experiments. The water molecules absorbed at the surface of the PVOH membranes, which decreased in amount as the temperature increased, resulted in drastic changes in molecular conformations on the surface of the membrane. At higher water contents (*i.e.*, lower pre-treatment temperatures), the relative band intensities of the hydroxyl groups and CH$_2$ bonds to the C−C bonds were less than the ratios determined at lower water content (*i.e.*, higher pre-treatment temperatures). However, after surface water was released at temperature above 60°C, the relative intensities of the (OH)/(C-H) bands remained constant as the temperature increased to approximately 110°C. The relative band intensities of these groups with respect to C-C bonds continued to decrease. According to the TGA results, constitutional water molecules remained present in the PVOH membranes in the temperature range 60 to 110°C (see Fig. 3). This observation indicated that the excitation of the less energetic mode associated to the C-C bonds was energetically favorable as the temperature increased relative to the modes assigned to the more energetic bands assigned to the OH groups and C-H bonds. The structural differences observed by Raman spectra as a function of temperature in the hydrated PVOH membrane had profound consequences on the proton transport. The dynamic ionic transport processes that were inferred from conductivity relaxation measurements that occurred at various temperature regions were different according to the water content of the membrane. The results were corroborated by DSC and TGA. This conclusion was also evident from the change observed in the shape of the relaxation peaks obtained from $M''(\omega)$ as a function of temperature. For example, the temperature dependence of the conductivity relaxation frequency, ω_{max}, followed different Arrhenius-type thermally activated processes at low temperatures compared to high temperatures. The corresponding activation energies in the two regions were 1.42 and 0.23 eV, respectively. Additionally, the selected fitting temperature regions and activation energies for the ω_{max} data were, (within experimental error), equivalent to the values obtained for $\sigma_0(T)$. This result strongly suggests that the mechanisms for long range ion displacement (*i.e.*, dc conductivity) and ion-ion or ion-polymer chain correlations were identical, (*i.e.*, ion-hoping) [23]. The presence of water molecules bound to the PVOH membrane at temperatures that favor OH-disorder (*i.e.*, in the absence water molecule), modified the proton-proton and proton-polymer chain interactions as determined by the conductivity relaxation measurements.

1. J.M.G. Cowie and S.H. Cree, *Annu. Rev. Phys. Chern.* **40** (1989) 85

2. V. S. Praptowidodo, *J. Molecular Structure* **739** (2005) 207.

3. Wei Zhang, Zhennan Zhang, and Xinping Wang, *J. Colloid and Interface Science* **333** (2009) 346.

4. Chun-Chen Yang, Sheng-Jen Lin, and Gwo-Mei Wu, *Mater. Chem. Phys.* **92** (2005) 251.

5. Arfat Anis, A.K. Banthia and S. Bandyopadhyay, *J. Materials Engineering and Performance* **17** (2008) 772

6. Li-Zhi Zhang, Yuang-Yuan Wang, Cai-Ling Wang, and Hui Zianng, *J. Membrane Sci.* **308** (2008) 198. Arfat Anis, A.K. Banthia and S. Bandyopadhyay, *J. Materials Engineering and Performance* **17** (2008) 772.

7. P. Balaji Bhargav, V. Madhu Mohan, and A.K. Sharma, *Ionics* **13** (2007) 173

8. M.A. Vargas Z. B-E. Mellander, and R.A. Vargas, *Physic. Status Solid B-Basic Research* **220** (2000) 615. M.A. Vargas, A. Garcia M., and R.A Vargas, *Electrochemical Acta* **43** (1998) 1271. M.A. Vargas, B-E. Mellander, and R.A. Vargas, *Electrochemical Acta* **45** (2000) 1399; J.H. Castillo, J.R, Castillo, M.N. Chacon, and R.A Vargas, *Ionics* **15** (2009) 537. R.A. Vargas, F. Bedoya, J.E. Castillo, L.A. Rodriguez, and M. Cachon, *J. Nanostructured Polymers And Nanocomposites* **6** (2010) 87.

9. Jen Ming Yang, Wen Yu Su, Te Lang Leu, and Ming Chein Yang, *J. Memebrane Science* **236** (2004) 39.

10. Z. Guo *et al*., *J. Nanopart. Res.* **12** (2010) 2415. S. Pyne *et al*., *J. Nanopart. Res.* **13** (2011).

11. D.S. Patil, J.S. Shaikh, D.S. Dalavi, S.S Kalagi, and P.S. Patil, *Mater. Chem. Phys.* **128** (2011) 449.

12. H. Mansur, Alexandra A.P. Mansur, *Mater. Chem. Phys.* **125** (2011) 709.

13. I.S. Elashmawi, N.A. Hakeem, and M. Soliman Selim, *Mater. Chem. Phys.* **115** (2009) 132

14. Young Moo Lee, Su Hwi Kim and Seon Jeong Kim, *Polymer* **26** (1996) 5897.

15. H. E. Assendert and A. H. Windle, *Polymer* **18** (1998) 4295.

16. I.A. Volegova, E.V. Konyukhova, and K. Godovsky, *J. Therm Anal Calorim.* **59** (2000) 123.

17. A. K. Jonscher, *Nature* **267** (1977) 673.

18. D.P Almond and A.R. West, *Nature* **306** (1983) 456. D.P Almond, G.K. Ducan, and A.R. West, *S. State Ionics* **8** (1983) 159; L. Marawski and R.J. Barczynski, *S. State Ionics* **176** (2005) 2145.

19. F. Funke, *Prog. Solid St. Chem.* **22** (1993) 111.

20. C.L. Londono-Calderón, C. Vargas-Hernandéz, and J.F.Jurado, *Rev. Mex. Fis* **56** (2011) 411. J. Jurado, C. Vargas-Hernández, and R.A. Vargas, *Rev. Mex. Fis.* **58** (2012) 411.

21. M. Ravi, Y. Pavani, K. Kiran Kumar, S. Bhavani, A.K. Sharma, and V.V.R. Narasimha Rao, *Mater. Chem. Phys.* **130** (2010) 442.

22. J. Ross Macdonald, *S. State Ionics* **176** (2005) 1961; D.P. Almond and A.R. West, *S. State Ionics* **11** (1983) 57.

23. M.A. Ahmed and M.S. Abo-Ellil, *J. Materials Science: Materials Electronics* **9** (1998) 391.

24. A.M. Shehap, *Egypt. J. Solids* **1** (2008) 75.

25. G. Socrates, *Infrared and Raman Characteristic Group Frequencies Tables and Charts*, (Thon Wiley & Sons, LTD, third edition, N.Y., 2004).